HHS Public Access

Author manuscript

Hepatology. Author manuscript; available in PMC 2016 May 01.

Published in final edited form as:

Hepatology. 2015 June ; 61(6): 1908–1919. doi:10.1002/hep.27719.

Activation of Aryl Hydrocarbon Receptor Dissociates Fatty Liver from Insulin Resistance by Inducing FGF21

Peipei Lu[1], **Jiong Yan**[1], **Ke Liu**[1], **Wojciech G. Garbacz**[1], **Pengcheng Wang**[1], **Meishu Xu**[1], **Xiaochao Ma**[1], and **Wen Xie**[1,2]

[1]Center for Pharmacogenetics and Department of Pharmaceutical Sciences, University of Pittsburgh, Pittsburgh, Pennsylvania

[2]Department of Pharmacology and Chemical Biology, University of Pittsburgh, Pittsburgh, Pennsylvania

Abstract

The aryl hydrocarbon receptor (AHR), also known as the dioxin receptor, was originally characterized as a xenobiotic receptor that senses xenotoxicants. Here we investigated the endobiotic and hepatic role of AHR in fatty liver and energy metabolism, and identified the endocrine factor that mediates the metabolic function of AHR. Wild type and liver-specific constitutively activated human AHR transgenic (TG) mice were used to investigate the role of AHR in fatty liver and energy homeostasis. Adenovirus expressing short hairpin RNA targeting the fibroblast growth factor 21 (FGF21) were used to determine the involvement of FGF21 in the metabolic effect of AHR. We showed that despite their severe fatty liver, the TG mice were protected from diet-induced obesity and type 2 diabetes. We identified the endocrine hormone FGF21 as a mediator for the metabolic benefit of AHR and established FGF21 as a direct transcriptional target of AHR. Interestingly, the transactivation of FGF21 by AHR contributed to both hepatic steatosis and systemic insulin hypersensitivity, both of which were largely abolished upon FGF21 knockdown.

Conclusions—The AHR-FGF21 endocrine signaling pathway establishes AHR as a pivotal environmental modifier that integrates signals from chemical exposure in the regulation of lipid and energy metabolism.

Keywords

Hepatic Steatosis; Diabetes; Dioxin; Gene Regulation; Transgenic Mice

Introduction

Environmental exposures to 2,3,7,8-tetrachlorodibenzo-*p*-dioxin (TCDD or dioxin), an agonist for the PAS domain transcriptional factor AHR, were associated with increased incidence of lipid abnormalities.(1) Highly expressed in the liver, AHR was initially recognized as a xenosensor that regulates xenobiotic metabolism. In recent years, the

Corresponding author: Dr. Wen Xie, Center for Pharmacogenetics, University of Pittsburgh, Pittsburgh, PA 15261, USA. wex6@pitt.edu.

endobiotic functions of AHR have been increasingly recognized, including our recent report that activation of AHR caused spontaneous hepatic steatosis.(2)

Hepatosteatosis is closely associated with insulin resistance, particularly in metabolic diseases.(3) On one hand, insulin resistance and the resultant hyperinsulinemia drives free fatty acid (FFA) influx to the liver by promoting lipolysis in peripheral adipose tissues and stimulates *de novo* lipogenesis.(4, 5) Liver fat accumulation, on the other hand, generates elevated levels of FFAs and pro-inflammatory lipid intermediates that disrupt insulin signaling and cause insulin resistance.(6) However, the causal relationship between steatosis and insulin resistance has been challenged.(7) Epidemiological studies revealed that subjects with the same level of hepatosteatosis can have either high or low insulin resistance.(8) Prolonged fasting in mice induced hepatosteatosis without causing insulin resistance.(9) In animal models, hepatosteatosis has been shown to be dissociated from insulin resistance, and even in some cases, hepatosteatosis was correlated with insulin hypersensitivity.(7) In the clinic, treatment of nonalcoholic fatty liver disease subjects with insulin-sensitizing agents often fails to relieve hepatosteatosis.(10)

Having known that activation of AHR causes spontaneous fatty liver,(2) it is paradoxical to note that TCDD induces the expression of fibroblast growth factor 21 (FGF21), a systemic insulin sensitizer.(11) FGF 21 is an atypical member of the FGF family produced predominantly in the liver.(12) FGF21 is induced by fasting through the activation of the peroxisome proliferator-activated receptor α (PPARα).(13, 14) FGF21 exhibits many metabolic benefits, ranging from reducing body weight to alleviation of hyperglycemia and insulin resistance, and improvement of lipid profiles.(15) Although FGF21 was shown to be regulated by TCDD, the pathophysiological relevance of this regulation remains undefined.

In this study, we demonstrated that activation of AHR dissociated fatty liver from insulin resistance by inducing FGF21. Specifically, the AHR transgenic mice were protected from high-fat diet (HFD)-induced obesity and insulin resistance despite having severe hepatosteatosis. The metabolic benefit of AHR was FGF21 dependent and FGF21 is a direct transcriptional target of AHR.

Materials and Methods

Mice and Diets

To generate the TetRE-CA-AHR transgenic mice, constitutively activated human AHR (CA-AHR) was constructed by deleting the human AHR region encoding the minimal ligand-binding domain (amino acids 273–432),(2) and then placed downstream of a minimal cytomegalovirus promoter fused to the tetracycline responsive element (TetRE). Pronuclear microinjection of the transgene into the C57BL/6 embryos was performed at the University of Pittsburgh Transgenic Core Facility. The TetRE-CA-AHR mice were bred with the FABP-tTA mice (16) to generate liver-specific FABP-CA-AHR mice. AHR knockout (AHRKO) mice in C57BL/6 background were purchased from Taconic (Hudson, NY). Mice were fed with standard chow from PMI Nutrition (St. Louis, MO) or HFD (S3282) from Bio-serv (Frenchtown, NJ). In the HFD model, 6-week-old mice received HFD for 12 weeks in most of the experiments, except that when adenovirus were used, mice were treated with

HFD for 6 weeks before viral infection. When necessary, doxycycline (DOX; 1 mg/ml) was given in drinking water. The food intake was measured for 7 days after 10 weeks of HFD feeding. Body composition was analyzed using EchoMRI-100TM from Echo Medical Systems (Houston, TX). The use of mice in this study complied with relevant federal guidelines and institutional policies.

Short Hairpin Adenoviral Production

Entry clones targeting either FGF21 or LacZ were gifts from Dr. Eleftheria Maratos-Flier.(13) To generate shRNA expression clones, FGF21 and LacZ entry vectors were used to perform LR recombination with the E1- and E3-deleted pAd/BLOCK-iT-DEST vector from Invitrogen. Adenoviruses were generated by transfecting 293A cells with vectors digested with PacI. After plaque selection and amplification, viruses were purified on a discontinuous CsCl gradient. Mice received adenovirus intravenously at the dose of 2×10^9 viral particle/g body weight.

Histological and Biochemical Analysis

For H&E staining, paraffin sections were stained with hematoxylin and eosin. For Oil Red O staining, snap-frozen liver tissues were sectioned at 8 μm and stained in 0.5% Oil Red O in propylene glycerol. Serum levels of triglyceride and cholesterol, ALT and AST (Stanbio Laboratory, Boerne, TX), insulin (Crystal Chem, Downers Grove, IL), IL-6, FGF21, and Adiponectin (R&D Systems, Minneapolis, MN) were measured by using commercial assay kits. To measure serum lipid levels, 75 μl of methanol was mixed with 25 μl of serum to extract lipids. To measure tissue lipid contents, tissues were homogenized and lipids were extracted in chloroform/methanol (2:1, v/v) as described.(16).

Indirect Calorimetry, Glucose Tolerance Test (GTT), and Insulin Tolerance Test (ITT)

Indirect calorimetry was performed using the Oxymax Indirect Calorimetry System (Columbus, OH). Mice were individually housed in the chamber with a 12 h light and 12 h dark cycle and monitored over a 48 h period. For GTT, mice were fasted for 12 h before receiving an intraperitoneal injection of D-glucose at 2 g/kg body weight. For ITT, mice were fasted for 6 h before receiving an intraperitoneal injection of insulin at 0.5 units/kg body weight.

Western Blotting Analysis

Tissues were lysed in RIPA buffer. Protein samples were resolved by SDS-PAGE gel, transferred to a polyvinylidene fluoride membrane. The primary antibodies used include those against AHR (N-19, Santa Cruz), pThr172AMPKα (cat# 2535, Cell Signaling) and total AMPKα (cat# 260, Cell Signaling), FGF21 (cat# 171941, Abcam), ApoB100 (H-15, Santa Cruz), and β-actin (A1978, Sigma).

Electrophoretic Mobility Shift Assay (EMSA), Chromatin Immunoprecipitation (ChIP) Assay, Transient Transfection and Luciferase Reporter Assay

EMSA was performed using ^{32}P-labeled oligonucleotides and in vitro synthesized receptor proteins.(16) ChIP assays for the human and mouse FGF21 promoters were performed on

293 cells transfected with pCMX-Flag-CA-AHR plasmid for 24 h and WT mice whose livers were transfected with the pCMX-Flag-CA-AHR plasmid by a hydrodynamic gene delivery method for 8 h,(16) respectively. Cell or liver lysates were immunoprecipitated with the anti-Flag antibody (Sigma).(16) The recovered DNA was assayed for enrichment of the FGF21 promoters by PCR. For luciferase reporter assay, the human FGF21 reporter plasmids (−2124/+29, −1836/+29, and −1562/+29) were PCR-amplified. The mouse FGF21 reporter plasmids (−98/+5 and −66/+5) were gifts from Dr. Steven A. Kliewer.(14) HepG2 cells were transfected with the reporter construct and AHR or CA-AHR expression vector in 48-well plates. When necessary, cells were treated with 3-methylcholanthrene (3-MC) (2 μM) or TCDD (10 nM) for 24 h before luciferase assay. The transfection efficiency was normalized against the β-galactosidase activities from a co-transfected CMX-β-galactosidase vector.

VLDL Secretion Assay

VLDL secretion rate *in vivo* was measured as described previously.(17) In brief, mice were fasted for 4 h before receiving an intravenous injection of tyloxapol at 500 mg/kg body weight. Tail vein blood samples were collected at 0, 60, and 90 min after the tyloxapol injection, and plasma triglyceride levels were measured.

Tissue Mitochondrial Fatty Acid Oxidation

Liver and skeletal muscle mitochondrial fatty acid oxidation was measured as described previously.(17) In brief, fresh tissues were placed in ice-cold modified Chappell-Perry buffer. Tissues were homogenized and mitochondria were isolated using differential centrifugation. Oxidation assays were performed using 0.2 mM [^{14}C]-oleate. Reactions were terminated by adding 100 μl of 70% perchloric acid, and [^{14}C]-CO_2 was trapped in 200 μL of 1 N NaOH. [^{14}C]-CO_2 and [^{14}C]-labeled acid-soluble metabolites were assessed by liquid scintillation counting.

Quantitative RT-PCR

Total RNA was extracted and subjected to reverse transcription with random hexamer primers and Superscript RT III enzyme (Invitrogen). SYBR Green-based qRT-PCR was performed with the ABI7500 System. Data were normalized against the cyclophilin control.

Statistical Analysis

Statistical significance was analyzed using an unpaired Student *t* test or analysis of variance (ANOVA) from GraphPad Prism (San Diego, CA). Differences were considered statistically significant at $P < 0.05$.

Results

Activation of AHR Exacerbated High-Fat Diet (HFD) Induced Steatosis

To study the *in vivo* function of human AHR, we generated the “Tet-off” transgenic mice overexpressing the constitutively activated human AHR (CA-AHR) in the liver under the control of fatty acid binding protein (FABP) gene promoter (Fig. 1A).(2) CA-AHR was

constructed by deleting the minimal ligand-binding domain of AHR.(18) The liver-specific expression of CA-AHR was confirmed at both mRNA and protein levels, without affecting the expression of endogenous AHR (Supplementary Fig. 1A). The expression of typical AHR target genes was induced in TG livers (Supplementary Fig. 1B). The gene regulatory effect appeared to be AHR specific and did not affect the activity of other partners of AHR nuclear translocator (ARNT), because the expression of VEGF, a typical target gene of the HIF1α-ARNT heterodimers, was not affected (Supplementary Fig. 1C). The transgene was not associated with hepatotoxicity, because neither the serum levels of liver injury markers (ALT, AST, and ALP) (Supplementary Fig. 1D) nor the expression of hepatic inflammatory cytokines or marker genes (Supplementary Fig. 1E) were increased in the TG mice. In chow-fed mice, the triglyceride, cholesterol, and fatty acid levels were increased, but the fed and fasting glucose levels were unchanged (Supplementary Fig. 2).

To determine whether AHR played a role in diet-induced fatty liver and associated metabolic syndrome, we challenged TG mice with HFD. Upon HFD feeding, the TG livers were larger and appeared paler and fattier compared to the WT livers (Fig. 1B). Hepatic triglyceride and cholesterol contents were higher (Fig. 1C, left panel), whereas serum levels of triglyceride and cholesterol were lower in TG mice (Fig. 1C, right panel). Interestingly, HFD feeding alone resulted in the accumulation of small lipid droplets within the hepatocytes of WT mice, whereas AHR activation caused formation of large lipid droplets as shown by H&E and Oil-red O staining (Fig. 1D). The small lipid droplets in WT liver were mainly localized in the central vein areas and were formed in almost all hepatocytes in that area, whereas the large lipid droplets in TG liver were mostly restricted to the portal vein areas and developed only in certain hepatocytes (Fig. 1D).

Hepatosteatosis is a result of imbalanced triglyceride secretion, *de novo* lipogenesis, fatty acid (FA) oxidation, or FA uptake.(19) The secretion of very-low-density lipoprotein (VLDL), which indicates the capacity of triglyceride secretion, was inhibited in HFD-fed TG mice (Fig. 1E, top panel). The protein level of ApoB100, the main structural component of VLDL, was reduced in TG liver (Fig. 1E, bottom panel). Interestingly, although it contained elevated concentrations of FFAs (Fig. 1F, left panel), the TG liver showed an unchanged rate of complete FA oxidation and a decreased rate of incomplete FA oxidation (Fig. 1F, middle panel), in which FAs entering the mitochondria are only partially degraded and may generate toxic metabolites that contribute to insulin resistance. The expression of fatty acid oxidation genes including Pparα and its targets Cpt1α, Lcad, and Mcad was decreased in TG liver (Fig. 1F, right panel), which was consistent with our previous report in transgenic mice expressing the constitutively activated mouse Ahr.(2) Despite their exacerbated steatosis, the TG mice showed a suppressed expression of lipogenic genes, including Srebp1c, Acc1, Scd1, and Fas (Fig. 1F, right panel).

AHR Transgenic Mice Were Protected from Diet-induced Obesity and Insulin Resistance

To our surprise, despite their exacerbated hepatosteatosis, the TG mice showed protection from diet-induced obesity and insulin resistance. Upon HFD feeding, the TG mice gained less body weight (Fig. 2A). At the end of the 12-week HFD feeding, TG mice were visibly leaner (Fig. 2B, left panel), and the lower body weight was accounted for largely by a

reduction in the fat mass without affecting the lean mass (Fig. 2B, right panel). The difference in adiposity was not attributable to a reduction in food intake (Fig. 2C). The TG mice had lower fasting glucose and insulin levels (Fig. 2D), as well as improved performance in GTT and ITT (Fig. 2E), suggesting an improved insulin sensitivity. These phenotypes seen in diet-induced mice were transgene dependent, because they were normalized in TG mice treated with doxycycline (DOX) to silence the transgene expression (Supplementary Fig. 3A-3C).

The Pleotropic Effects of AHR in Improving Metabolic Function

Although the AHR transgene was targeted to the liver, we observed metabolic benefits in extrahepatic tissues, including adipose tissues and skeletal muscle. Obesity is associated with an increase in macrophage infiltration in adipose tissue.(20) Consistent with their reduced size of visceral fat pad (Fig. 3A, left panel), the HFD-fed TG mice showed smaller adipocyte size and lower macrophage infiltration as shown by less crown-like structures (Fig. 3A, middle panel), which was supported by their decreased expression of macrophage marker genes (Fig. 3A, right panel).

Reduction in fat mass without affecting food intake suggested an increase in energy expenditure. Indeed, both the oxygen consumption (Fig. 3B, left panel) and energy expenditure (Fig. 3B, middle panel) were significantly higher in TG mice, which were normalized upon DOX treatment (Supplementary Fig. 3D). There was also an increase in the resting rectal temperature in TG mice (Fig. 3B, right panel), another indicator of increased energy expenditure and thermogenesis. The brown adipose tissue (BAT) plays an important role in thermogenesis. The TG BAT was obviously browner (Fig. 3C, left panel), which was supported by smaller adipocytes with smaller lipid droplets (Fig. 3C, middle panel), and increased expression of BAT marker genes Dio2, Cidea and Elovl3 (Fig. 3C, right panel). We also observed an increased serum level and adipose expression of adiponectin (Fig. 3D), an adipokine known to have anti-inflammatory and insulin sensitizing effects.(21)

AMP-activated protein kinase (AMPK) is a key player in regulating energy metabolism.(22) We observed an elevated AMPKα phosphorylation in the liver and skeletal muscle, but not the white adipose tissue (WAT), of TG mice (Fig. 3E), which was normalized upon DOX treatment (Supplementary Fig. 3E). AMPK activation is known to promote fatty acid oxidation in the skeletal muscle.(23) Indeed, the complete fatty acid oxidation rate in TG muscle was significantly increased (Fig. 3F, left panel), which was associated with an increased expression of Pgc1α, Cpt1α and Ucp3 (Fig. 3F, right panel).

Activation of AHR Induced the Expression of FGF21, and Knockdown of FGF21 Abolished the Metabolic Benefits of AHR

The pronounced dissociation of hepatosteatosis from insulin resistance and the pleotropic metabolic benefits in our TG mice prompted us to examine the underlying mechanism. We found that both the hepatic mRNA and protein expression and circulating concentration of FGF21 were significantly increased in both the chow-fed and HFD-fed TG mice (Fig. 4A). The FGF21 induction was liver-specific, because the induction was not seen in WAT and

BAT (Fig. 4B). The serum level and hepatic expression of FGF21 in the TG mice were normalized upon DOX treatment (Supplementary Fig. 4).

To understand the functional relevance of FGF21 induction, WT and TG mice were fed with HFD for 6 weeks before receiving an intravenous injection of adenovirus expressing short hairpin RNA targeting FGF21 (Ad-shFGF21) or the control LacZ gene (AdshLacZ).(13) The FGF21 knockdown was validated (Fig. 4C). Although the lower body weight (Fig. 4D) and decreased WAT mass (data not shown) of TG mice were not affected, FGF21 knockdown abolished the transgenic effects in lowering fasting glucose levels (Fig. 4E) as well as improving glucose tolerance (Fig. 4F).

Upon FGF21 knockdown, the extrahepatic benefits of the transgene were also abolished. These included the decreased WAT macrophage infiltration (Fig. 5A) and decreased WAT expression of pro-inflammatory cytokines and macrophage marker genes (Fig. 5B), browning of the BAT (Fig. 5C) and increased expression of BAT marker genes (Fig. 5D), and increased serum level of adiponectin (Fig. 5E). In the skeletal muscle, the increased complete fatty acid oxidation (Fig. 5F, left panel) and elevation of AMPKα phosphorylation (Fig. 5E, right panel) were largely attenuated by FGF21 knockdown.

FGF21 Knockdown Ameliorated Hepatosteatosis but Exacerbated Liver Damage in TG Mice

Interestingly, the large lipid droplets in HFD-fed TG livers were depleted upon FGF21 knockdown (Fig. 6A), although the knockdown did not affect the repression of VLDL secretion (Fig. 6B). The elevated hepatic triglyceride and cholesterol contents were decreased after FGF21 knockdown (Fig. 6C), which was associated with increased serum levels of triglycerides and cholesterol (Fig. 6C). Consistent with the decreased lipd droplet size, the induction of several lipid droplet-associated genes observed in shLacZ-infected TG mice, including Plin1, Plin3, and Cidec, was decreased in shFGF21-infected TG mice (Fig. 6D). The hepatic FFA concentrations (Fig. 6E, left panel) and fatty acid oxidation rate (Fig. 6E, right two panels) in TG mice were not affected by FGF21 knockdown.

Paradoxically, the depleted lipid droplets in shFGF21-infected TG livers was associated with hepatotoxicity as supported by increased hepatocyte degeneration and lymphocyte infiltration (Fig. 6A), increased expression of pro-inflammatory genes (Fig. 6F, left panel), and increased serum levels of IL-6 (Fig. 6F, middle panel) and ALT (Fig. 6F, right panel). The hepatic concentrations of diacylglycerol and ceramide, two lipotoxic lipid intermediates,(24, 25), were not affected in TG mice (data not shown).

FGF21 is a Direct Transcriptional Target of AHR

The induction of FGF21 was also observed in WT mice acutely treated with TCDD, which was abolished in AHRKO mice (Fig. 7A). These results, together with the FGF21 induction in TG mice, strongly suggested FGF21 as an AHR target gene. We cloned the human and mouse FGF21 gene promoters and evaluated their regulation by AHR. Inspection of the promoters revealed two putative dioxin responsive elements (DREs) in the hFGF21 gene promoter and one DRE in the mFGF21 gene promoter, whose bindings to the AHR-ARNT heterodimers or the CA-AHR-ARNT heterodimers were confirmed by EMSA (Fig. 7B). To

confirm the recruitment of CA-AHR onto the hFGF21 gene promoter *in vivo*, we performed ChIP assay on cells transfected with Flag-CA-AHR. As shown in Fig. 7C, CA-AHR specifically recruited to the two DRE-franking regions, but not the control non-DRE region. The *in vivo* recruitment of CA-AHR onto the mFGF21 gene promoter was confirmed by ChIP assay in WT mice whose livers were transfected with Flag-CA-AHR (Fig. 7D). The transactivation of the FGF21 gene promoters by AHR was evaluated by luciferase reporter gene assays. As shown in Fig. 7E, the 2-kb hFGF21 gene promoter was transactivated by CA-AHR or AHR in the presence of the AHR agonist 3-MC, whereas this activation was abolished when the region containing both DREs was deleted. A similar pattern of results was obtained when the mFGF21 gene promoter was evaluated (Fig. 7F).

Discussion

The most interesting finding is the revelation of the AHR-FGF21 pathway and the implication of this regulation in conferring the metabolic benefit of AHR. FGF21 is known to have multiple metabolic benefits including reducing body weight and improving insulin sensitivity.(15) We showed the induction of FGF21 was transgene specific, because silencing of the transgene normalized the induction and attenuated the metabolic benefit. We also showed, through the FGF21 knockdown, that FGF21 was required for the metabolic benefit of the transgene. The increased circulating level of FGF21 may have explained the pleotropic and extrahepatic benefits of the liver-specific AHR activation, such as those observed in the adipose tissues and skeletal muscle. The increased adipose expression and circulating level of adiponectin in TG mice were consistent with the notion that adiponectin mediates the systemic effects of FGF21 on energy metabolism and insulin sensitivity.(26) The AMPKα phosphorylation in the liver and skeletal muscle of TG mice was increased, consistent with the report that FGF21 regulates energy homeostasis through the activation of AMPK.(27) Although FGF21 expression can be regulated by PPARα,(13, 14) the hepatic expression of PPARα and its downstream target genes was down-regulated in TG mice, suggesting that PPARα was unlikely the mediator for the FGF21 induction in our mice. Although FGF21 was established as an AhR target gene, the basal and fasting-inducible expression of FGF21 was not affected in AhRKO mice (data not shown), suggesting that PPARα may have played a dominating role in maintaining the basal and fasting-inducible FGF21 expression.

Another intriguing finding is the dissociation between hepatosteatosis and insulin resistance in our TG mice. Although paradoxically, several recent studies suggested that hepatosteatosis and insulin resistance can be dissociated. For example, liver-specific knockout of the histone deacetylase 3 improved insulin sensitivity despite the hepatosteatosis.(28) In another example, overexpressing the acyl-CoA:diacylglycerol acyltransferase 2 in the liver increased lipid accumulation without developing insulin resistance.(29) One possibility that accounts for the dissociation is that insulin resistance may reflect inflammation rather than lipid accumulation in the liver.(30) Indeed, there was no sign of inflammation in the TG liver despite the elevated lipid contents, suggesting that these lipids are sequestered in lipid droplets and thus prevented from causing lipotoxicity. In contrast, knockdown of FGF21 may have resulted in rupture of lipid droplets, leading to liver inflammation and toxicity, as well as the masking of insulin hypersensitivity. Our

results suggested that in the context of AHR activation, FGF21 may have promoted lipid sequestration and storage into lipid droplets by up-regulating the expression of lipid droplet-associated genes (Fig. 6C), the mechanism of which remains to be understood. Decreased hepatic lipid contents were accompanied by increased serum triglyceride and cholesterol levels in FGF21-depleted TG mice, suggesting that liver fat is redistributed to the peripheral.

The lack of increased hepatic fatty acid oxidation in HFD-fed TG mice seemed contradictory to the known function of FGF21 in promoting fatty acid oxidation and tricarboxylic acid cycle flux in the liver.(31, 32) However, our TG mice also showed decreased expression of PPARα and other fatty acid oxidation genes, which was consistent with those observed in transgenic mice expressing the constitutively activated mouse Ahr. (2) The mechanism by which AHR supresses faty acid oxidation is unclear. Nevertheless, we reasoned the decreased incomplete oxidation and unchanged complete oxidation were the net result of the opposing effect of FGF21 and AHR on fatty acid oxidation. The absence of change in hepatic fatty acid oxidation after FGF21 knockdown also suggested a limited effect of FGF21 on hepatic fatty acid oxidaiton in our TG mice.

AHR was initially defined as a xenobiotic receptor that regulates drug metabolism. Subsequent observations, such as the developmental defects in AHR null mice(33, 34) and identification of endogenous AHR ligands(35, 36) have suggested equally important endobiotic functions of AHR. More recent studies suggested AHR also plays many other essential biological functions, such as functioning as an E3 ligase(37) and affecting the expansion of human hematopoietic stem cells.(38). Our results suggested that endogenous AhR ligands may play a role in regulating FGF21 and energy metabolism. AHR can also be activated by numerous xenobiotic ligands. However, the *in vivo* effect of xenobiotic AhR ligands on energy metabolism is yet to be tested, a major challenge of which is to avoid drug toxicity. The typical pharmacological model of AHR activation using TCDD is often associated with toxicity that may affect the data interpretation, especially when the ligand has to be used chronically. Our TG mice offers a unique gain of function model to understand the endobiotic function of AHR without the concern of the toxicity.

In summary, we showed that transgenic activation of AHR in the liver alleviated mice from HFD-induced obesity and insulin resistance despite having marked hepatosteatosis. The dissociation between fatty liver and insulin resistance likley has been mediated by the AHR-dependent activation of FGF21. We propose the endocrine hormone FGF21 as an important effector for the endobiotic function of AHR in lipid metabolism and energy homeostasis. Our results also suggest that development of non-toxic AHR agonists may be a novel approach to manage metabolic syndrome.

Supplementary Material

Refer to Web version on PubMed Central for supplementary material.

Acknowledgements

The authors thank Dr. Eleftheria Maratos-Flier (Beth Israel Deaconess Medical Center) for the entry clones encoding shRNA agaisnt FGF21 and LacZ, Dr. Steven A. Kliewer (UT Southwestern Medical Center) for the

mouse FGF21 luciferase reporters, and Dr. Robert O'Doherty (University of Pittsburgh) for the use of metabolic cages.

Financial Support: This work was supported in part by NIH grants DK083952 and HD073070 to WX.

Abbreviations

AHR	aryl hydrocarbon receptor
AHRKO	AHR knockout
AMPK	AMP-activated protein kinase
ARNT	AHR nuclear translocator
BAT	brown adipose tissue
DOX	doxycycline
DRE	dioxin responsive element
FABP	fatty acid binding protein
FFA	free fatty acid
FGF21	fibroblast growth factor 21
HFD	high-fat diet
NAFLD	nonalcoholic fatty liver disease
PPARα	peroxisome proliferator-activated receptor α
TCDD	2,3,7,8-tetrachlorodibenzo-*p*-dioxin
WAT	white adipose tissue

References

1. Remillard RB, Bunce NJ. Linking dioxins to diabetes: epidemiology and biologic plausibility. Environ Health Perspect. 2002; 110:853–858. [PubMed: 12204817]
2. Lee JH, Wada T, Febbraio M, He J, Matsubara T, Lee MJ, et al. A novel role for the dioxin receptor in fatty acid metabolism and hepatic steatosis. Gastroenterology. 2010; 139:653–663. [PubMed: 20303349]
3. Utzschneider KM, Kahn SE. Review: The role of insulin resistance in nonalcoholic fatty liver disease. The Journal of clinical endocrinology and metabolism. 2006; 91:4753–4761. [PubMed: 16968800]
4. Postic C, Girard J. Contribution of de novo fatty acid synthesis to hepatic steatosis and insulin resistance: lessons from genetically engineered mice. J Clin Invest. 2008; 118:829–838. [PubMed: 18317565]
5. Browning JD, Horton JD. Molecular mediators of hepatic steatosis and liver injury. J Clin Invest. 2004; 114:147–152. [PubMed: 15254578]
6. Shoelson SE, Lee J, Goldfine AB. Inflammation and insulin resistance. J Clin Invest. 2006; 116:1793–1801. [PubMed: 16823477]
7. Sun Z, Lazar MA. Dissociating fatty liver and diabetes. Trends Endocrinol Metab. 2013; 24:4–12. [PubMed: 23043895]
8. Stefan N, Kantartzis K, Haring HU. Causes and metabolic consequences of Fatty liver. Endocrine Reviews. 2008; 29:939–960. [PubMed: 18723451]

9. Heijboer AC, Donga E, Voshol PJ, Dang ZC, Havekes LM, Romijn JA, Corssmit EP. Sixteen hours of fasting differentially affects hepatic and muscle insulin sensitivity in mice. J Lipid Res. 2005; 46:582–588. [PubMed: 15576835]
10. Uygun A, Kadayifci A, Isik AT, Ozgurtas T, Deveci S, Tuzun A, et al. Metformin in the treatment of patients with non-alcoholic steatohepatitis. Alimentary pharmacology & therapeutics. 2004; 19:537–544. [PubMed: 14987322]
11. Lu H, Cui W, Klaassen CD. Nrf2 protects against 2,3,7,8-tetrachlorodibenzo-p dioxin (TCDD)-induced oxidative injury and steatohepatitis. Toxicol Appl Pharmacol. 2011; 256:122–135. [PubMed: 21846477]
12. Kliewer SA, Mangelsdorf DJ. Fibroblast growth factor 21: from pharmacology to physiology. Am J Clin Nutr. 2010; 91:254S–257S. [PubMed: 19906798]
13. Badman MK, Pissios P, Kennedy AR, Koukos G, Flier JS, Maratos-Flier E. Hepatic fibroblast growth factor 21 is regulated by PPARalpha and is a key mediator of hepatic lipid metabolism in ketotic states. Cell Metab. 2007; 5:426–437. [PubMed: 17550778]
14. Inagaki T, Dutchak P, Zhao G, Ding X, Gautron L, Parameswara V, et al. Endocrine regulation of the fasting response by PPARalpha-mediated induction of fibroblast growth factor 21. Cell Metab. 2007; 5:415–425. [PubMed: 17550777]
15. Kharitonenkov A, Shiyanova TL, Koester A, Ford AM, Micanovic R, Galbreath EJ, et al. FGF-21 as a novel metabolic regulator. J Clin Invest. 2005; 115:1627–1635. [PubMed: 15902306]
16. Zhou J, Zhai Y, Mu Y, Gong H, Uppal H, Toma D, et al. A novel pregnane X receptor-mediated and sterol regulatory element-binding protein-independent lipogenic pathway. J Biol Chem. 2006; 281:15013–15020. [PubMed: 16556603]
17. Gao J, He J, Zhai Y, Wada T, Xie W. The constitutive androstane receptor is an anti-obesity nuclear receptor that improves insulin sensitivity. J Biol Chem. 2009; 284:25984–25992. [PubMed: 19617349]
18. McGuire J, Okamoto K, Whitelaw ML, Tanaka H, Poellinger L. Definition of a dioxin receptor mutant that is a constitutive activator of transcription: delineation of overlapping repression and ligand binding functions within the PAS domain. J Biol Chem. 2001; 276:41841–41849. [PubMed: 11551926]
19. Cohen JC, Horton JD, Hobbs HH. Human fatty liver disease: old questions and new insights. Science. 2011; 332:1519–1523. [PubMed: 21700865]
20. Weisberg SP, McCann D, Desai M, Rosenbaum M, Leibel RL, Ferrante AW Jr. Obesity is associated with macrophage accumulation in adipose tissue. J Clin Invest. 2003; 112:1796–1808. [PubMed: 14679176]
21. Maeda N, Shimomura I, Kishida K, Nishizawa H, Matsuda M, Nagaretani H, et al. Diet-induced insulin resistance in mice lacking adiponectin/ACRP30. Nat Med. 2002; 8:731–737. [PubMed: 12068289]
22. Zhang BB, Zhou G, Li C. AMPK: an emerging drug target for diabetes and the metabolic syndrome. Cell Metab. 2009; 9:407–416. [PubMed: 19416711]
23. Lee WJ, Kim M, Park HS, Kim HS, Jeon MJ, Oh KS, et al. AMPK activation increases fatty acid oxidation in skeletal muscle by activating PPARalpha and PGC-1. Biochem Biophys Res Commun. 2006; 340:291–295. [PubMed: 16364253]
24. Erion DM, Shulman GI. Diacylglycerol-mediated insulin resistance. Nat Med. 2010; 16:400–402. [PubMed: 20376053]
25. Summers SA. Ceramides in insulin resistance and lipotoxicity. Prog Lipid Res. 2006; 45:42–72. [PubMed: 16445986]
26. Lin Z, Tian H, Lam KS, Lin S, Hoo RC, Konishi M, et al. Adiponectin mediates the metabolic effects of FGF21 on glucose homeostasis and insulin sensitivity in mice. Cell Metab. 2013; 17:779–789. [PubMed: 23663741]
27. Chau MD, Gao J, Yang Q, Wu Z, Gromada J. Fibroblast growth factor 21 regulates energy metabolism by activating the AMPK-SIRT1-PGC-1alpha pathway. Proc Natl Acad Sci U S A. 2010; 107:12553–12558. [PubMed: 20616029]

28. Sun Z, Miller RA, Patel RT, Chen J, Dhir R, Wang H, et al. Hepatic Hdac3 promotes gluconeogenesis by repressing lipid synthesis and sequestration. Nat Med. 2012; 18:934–942. [PubMed: 22561686]
29. Monetti M, Levin MC, Watt MJ, Sajan MP, Marmor S, Hubbard BK, et al. Dissociation of hepatic steatosis and insulin resistance in mice overexpressing DGAT in the liver. Cell Metab. 2007; 6:69–78. [PubMed: 17618857]
30. Arkan MC, Hevener AL, Greten FR, Maeda S, Li ZW, Long JM, et al. IKK-beta links inflammation to obesity-induced insulin resistance. Nat Med. 2005; 11:191–198. [PubMed: 15685170]
31. Potthoff MJ, Inagaki T, Satapati S, Ding X, He T, Goetz R, et al. FGF21 induces PGC-1alpha and regulates carbohydrate and fatty acid metabolism during the adaptive starvation response. Proc Natl Acad Sci U S A. 2009; 106:10853–10858. [PubMed: 19541642]
32. Fisher FM, Chui PC, Nasser IA, Popov Y, Cunniff JC, Lundasen T, et al. Fibroblast Growth Factor 21 Limits Lipotoxicity by Promoting Hepatic Fatty Acid Activation in Mice on Methionine and Choline-deficient Diets. Gastroenterology. 2014
33. Fernandez-Salguero PM, Hilbert DM, Rudikoff S, Ward JM, Gonzalez FJ. Aryl hydrocarbon receptor-deficient mice are resistant to 2,3,7,8-tetrachlorodibenzo-p-dioxin-induced toxicity. Toxicol Appl Pharmacol. 1996; 140:173–179. [PubMed: 8806883]
34. Schmidt JV, Su GH, Reddy JK, Simon MC, Bradfield CA. Characterization of a murine Ahr null allele: involvement of the Ah receptor in hepatic growth and development. Proc Natl Acad Sci U S A. 1996; 93:6731–6736. [PubMed: 8692887]
35. Beischlag TV, Luis Morales J, Hollingshead BD, Perdew GH. The aryl hydrocarbon receptor complex and the control of gene expression. Crit Rev Eukaryot Gene Expr. 2008; 18:207–250. [PubMed: 18540824]
36. Nguyen LP, Bradfield CA. The search for endogenous activators of the aryl hydrocarbon receptor. Chem Res Toxicol. 2008; 21:102–116. [PubMed: 18076143]
37. Ohtake F, Baba A, Takada I, Okada M, Iwasaki K, Miki H, et al. Dioxin receptor is a ligand-dependent E3 ubiquitin ligase. Nature. 2007; 446:562–566. [PubMed: 17392787]
38. Boitano AE, Wang J, Romeo R, Bouchez LC, Parker AE, Sutton SE, et al. Aryl hydrocarbon receptor antagonists promote the expansion of human hematopoietic stem cells. Science. 2010; 329:1345–1348. [PubMed: 20688981]

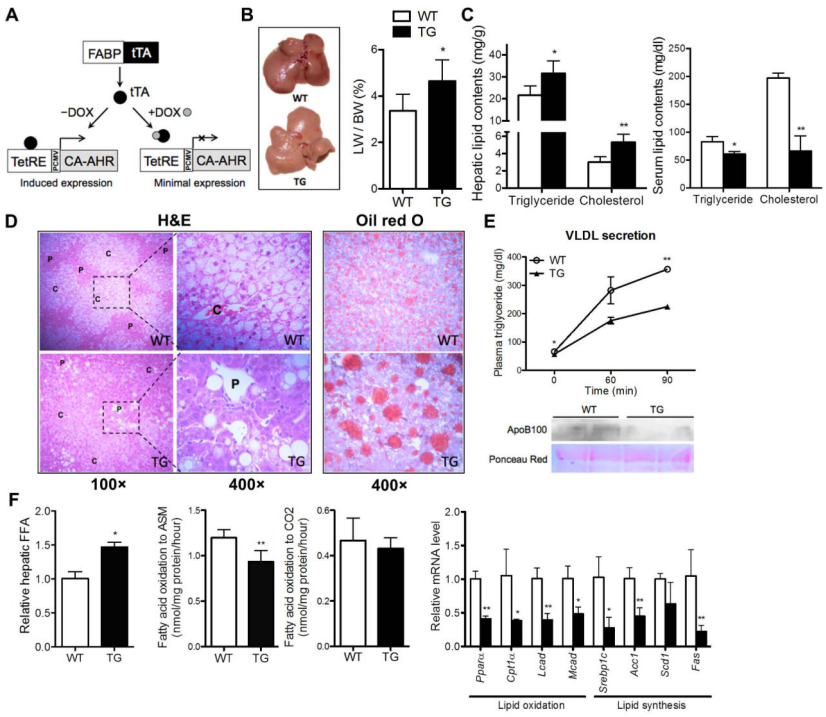

Fig. 1. Activation of AHR exacerbated high-fat diet induced steatosis

(A) Schematic presentation of the Tet-off FABP-tTA/TetRE-CA-AHR transgenic system. P_{CMV}, minimal cytomegalovirus promoter. **(B to F)** Mice were fed with HFD for 12 weeks. Shown are the gross appearance of the livers (left) and liver weight to body weight ratio (right) (B); hepatic (left) and serum (right) triglyceride and cholesterol contents (C); H&E staining (left) and Oil-red staining (right) of the liver sections (D); VLDL secretion rate (top) and Western blotting of serum ApoB100 (bottom) (E); and hepatic free fatty acid (FFA) contents (left), incomplete fatty acid oxidation of [^{14}C]-oleate to acid-soluble metabolite (ASM) and complete fatty acid oxidation of [^{14}C]-oleate to CO_2 in liver homogenates (middle), and mRNA expressions of lipid oxidation genes and lipogenic genes (right) (F). N=5 for each group. *, P<0.05; **, P<0.01. TG vs. WT.

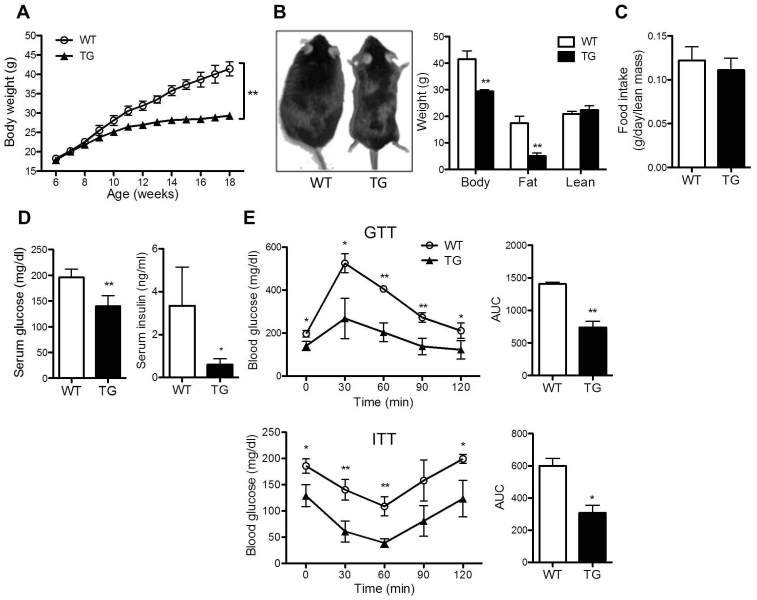

Fig. 2. AHR transgenic mice were protected from diet-induced obesity and insulin resistance

Mice were same as described in Fig. 1. **(A)** Growth curve of mice. **(B)** Appearance of mice (left) and body composition (right) at the end of HFD feeding. **(C)** Food intake. **(D)** Fasting serum glucose and insulin levels. **(E)** Glucose tolerance test (GTT) (top) and insulin tolerance test (ITT) (bottom) and their quantification presented as area under curve (AUC). N=5 for each group. *, $P<0.05$; **, $P<0.01$.

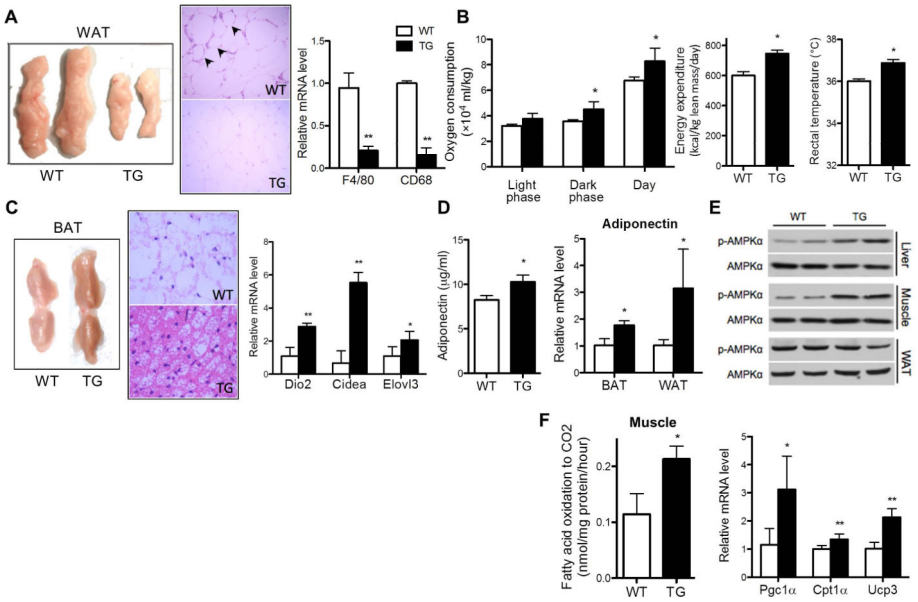

Fig. 3. The pleotropic effects of AHR in improving metabolic function

Mice were same as described in Fig. 1. **(A)** Representative appearance (left) and H&E staining (middle) of visceral fat tissues, and the white adipose tissue (WAT) expression of macrophage markers (right). Arrowheads indicate the crown-like structures. **(B)**Measurements of oxygen consumption (left), energy expenditure (middle), and rectal tempeature (right). **(C)** Representative appearance (left) and H&E staining (middle) of brown fat tissue (BAT), and BAT expression of brown markers (right). **(D)** Serum adiponectin level (left) and adipose expression of adiponectin (right). **(E)** Western blotting of p-AMPKα and total AMPKα. **(F)** Complete fatty acid oxidation of [^{14}C]-oleate to CO_2 in skeletal muscle (left) and muscular expression of β-oxidation genes (right). N=5 for each group. *, P<0.05; **, P<0.01.

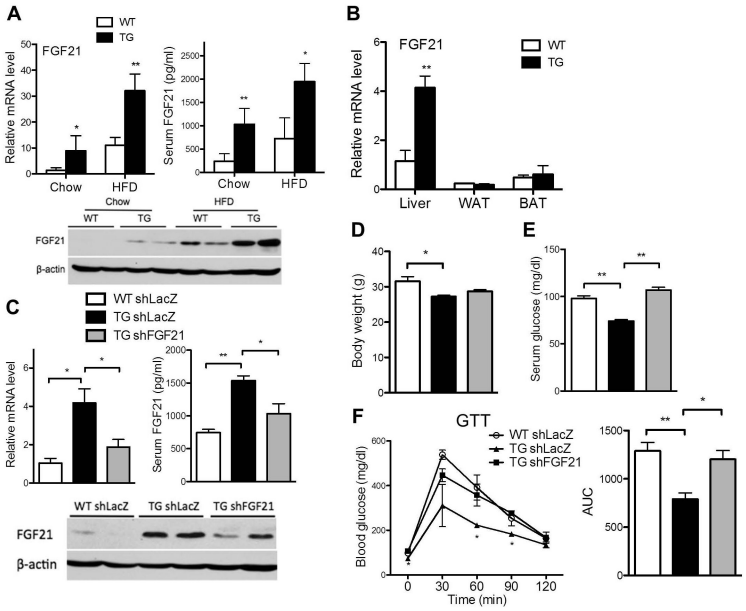

Fig. 4. Activation of AHR induced the expression of FGF21, and knockdown of FGF21 abolished the metabolic benefits of AHR

(A) Mice were fed with chow diet for 6 weeks or HFD for 12 weeks. Hepatic mRNA expression (top left), serum level (top right), and Western blotting (bottom) of FGF21. **(B)** mRNA expression of FGF21 in tissues of mice fed with HFD for 12 weeks. **(C to F)** Mice were fed with HFD for 6 weeks before receiving Ad-shFGF21 or Ad-shLacZ for one week. Shown are hepatic mRNA expression (top left), serum level (top right), and Western blotting (bottom) of FGF21 (C); body weight (D); fasting serum glucose level (E); and glucose tolerance test (GTT) and its quantification (F). N=4 for each group. *, $P<0.05$; **, $P<0.01$, TG vs. WT, or the comparisons are labled.

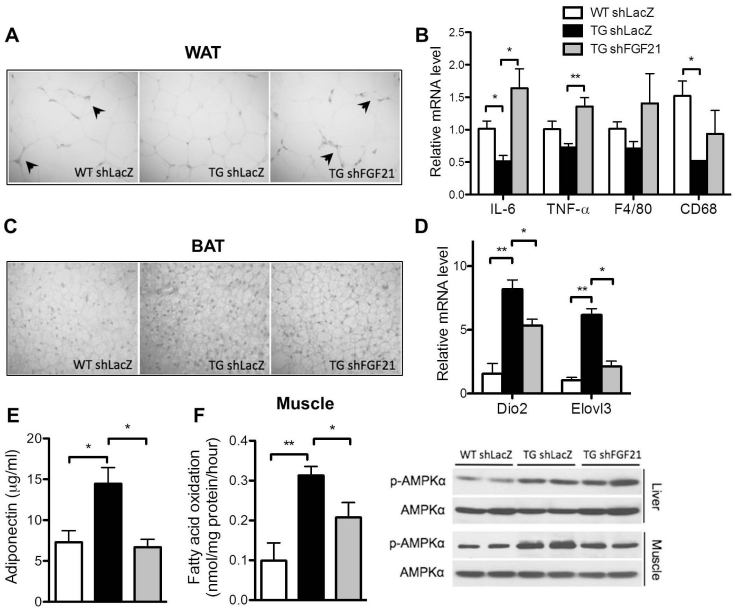

Fig. 5. Knockdown of FGF21 abolished the metabolic benefits of AHR in extrahepatic tissues

Mice were same as described in Fig. 4C. **(A and B)** H&E staining (A) and expression of inflammatory marker genes (B) in WAT. Arrowheads indicate the crown-like structures. **(C and D)** H&E staining (C) and expression of brown markers (D) in BAT. **(E)** Serum adiponectin levels (left). **(F)** Complete fatty acid oxidation in skeletal muscle (left panel) and Western blotting of p-AMPKα and total AMPKα (right). N=4 for each group. *, $P<0.05$; **, $P<0.01$.

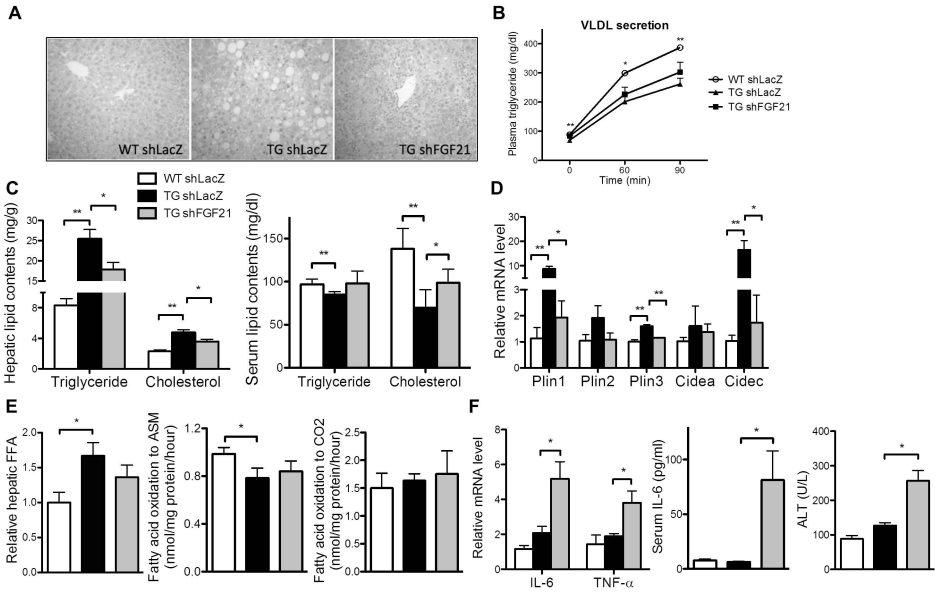

Fig. 6. FGF21 knockdown ameliorated hepatosteatosis but exacerbated liver damage in TG mice

Mice were same as described in Fig. 4C. **(A and B)** H&E staining of liver tissues (A) and VLDL secretion rate (B). **(C)** Hepatic (left) and serum (right) triglyceride and cholesterol contents. **(D)** Hepatic mRNA expression of lipid droplet associated genes. **(E)** Hepatic free fatty acid (FFA) contents (left), incomplete fatty acid oxidation of [^{14}C]-oleate to acid-soluble metabolite (ASM) (middle), and complete fatty acid oxidation of [^{14}C]-oleate to CO_2 in liver homogenates (right). **(F)** Hepatic mRNA expression of pro-inflammatory cytokines (left) and serum levels of IL-6 (right) and ALT (right). N=4 for each group. *, P<0.05; **, P<0.01, TG shLacZ vs. WT shLacZ, or the comparisons are labled.

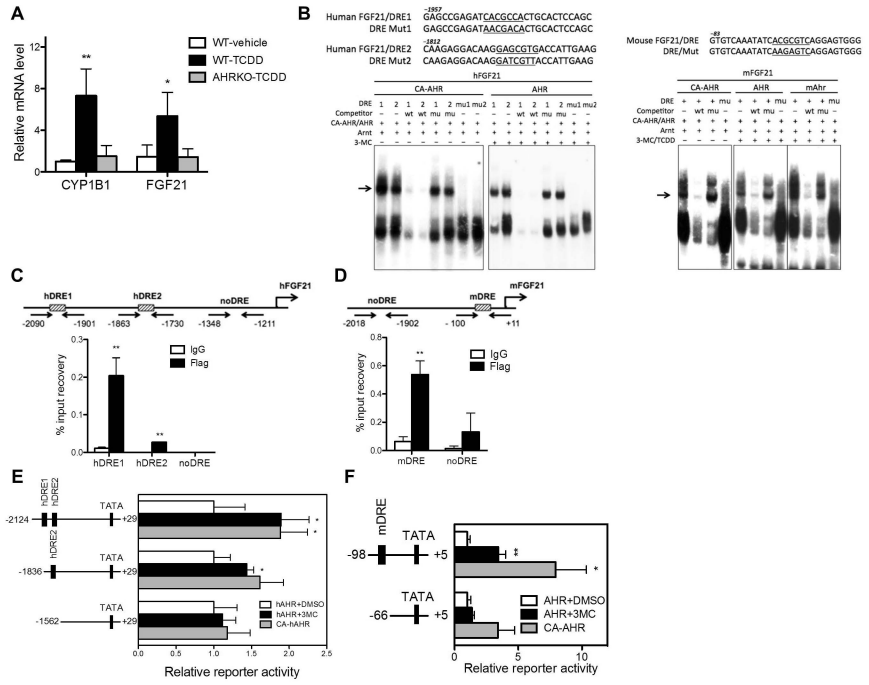

Fig. 7. FGF21 is a direct transcriptional target of AHR

(A) Eight-week old WT and AHR knockout (AHRKO) mice were treated with a single dose of TCDD (30 μg/kg) and sacrificed 4 h later. The hepatic mRNA expression of CYP1B1 and FGF21 was measured by real-time PCR. **(B)** The sequences of human and mouse FGF21 DREs and their mutant variants (top) and EMSA results (bottom). **(C and D)** ChIP assay to show the recruitment of CA-AHR onto the human (C) and mouse (D) FGF21 promoters. 293 cells were transfected with pCMX-Flag-CA-AHR in (C) and WT mouse livers were hydrodynamically transfected with pCMX-Flag-CA-AHR in (D). **(E and F)** Activation of the human (E) and mouse (F) FGF21 promoter reporter genes by AHR in the presence of 3-methylcholanthrene (3-MC), or by CA-AHR without an exogenously added ligand. HepG2 cells were co-transfected with indicated reporters and receptors. Transfected cells were treated with vehicle DMSO or 3-MC (2 μM) for 24 h before luciferase assay. *, $P<0.05$; **, $P<0.01$.